＜経時的発現変動を示す遺伝子の抽出＞

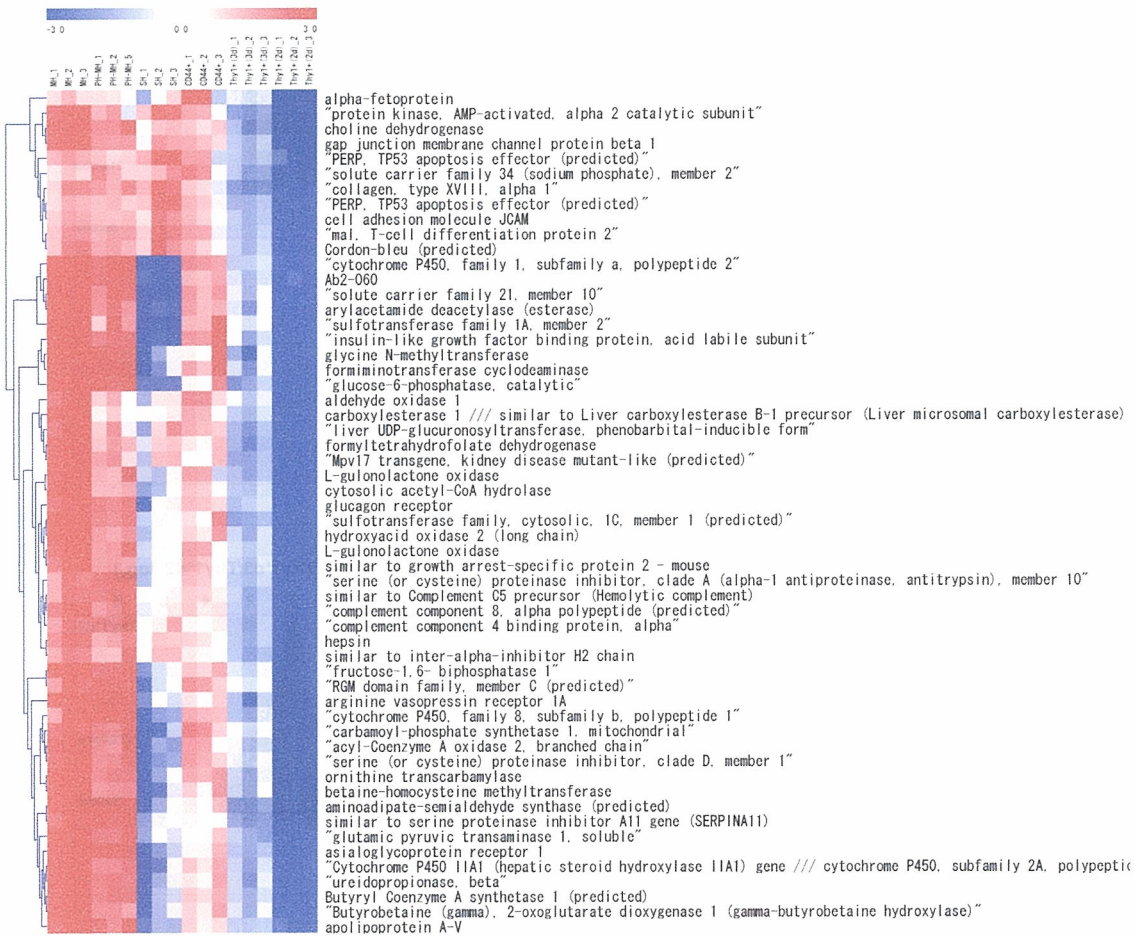

Thy1+(3d)/Thy1+(2d)>4 かつ CD44+/Thy1(3d)>4 であるプローブ（数値は相対値）

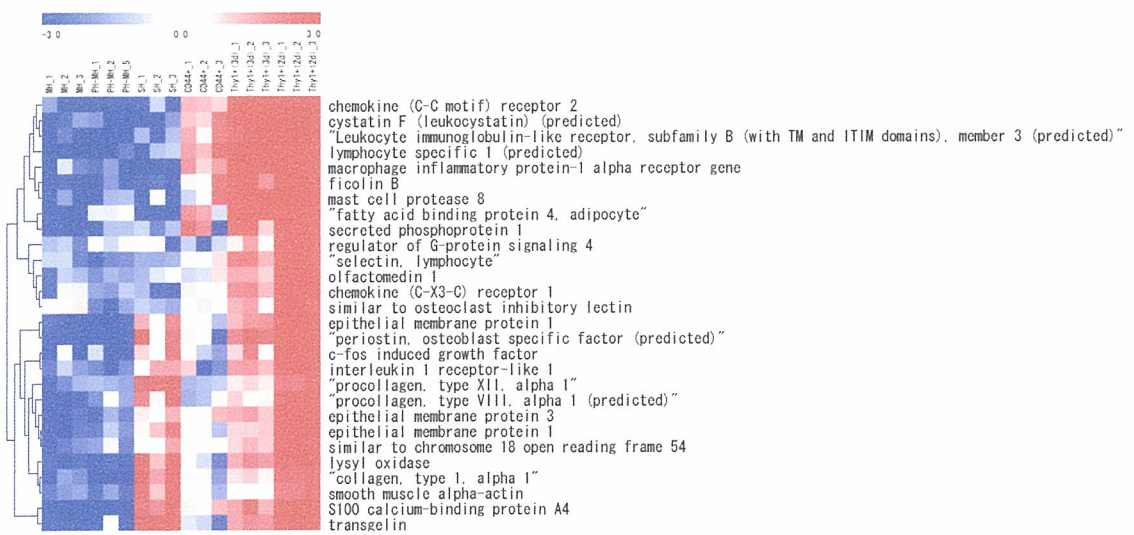

Thy1+(3d)/Thy1+(2d)<0.5 かつ CD44+/Thy1(3d)<0.5 であるプローブ（数値は相対値）

＜Pathway 解析＞

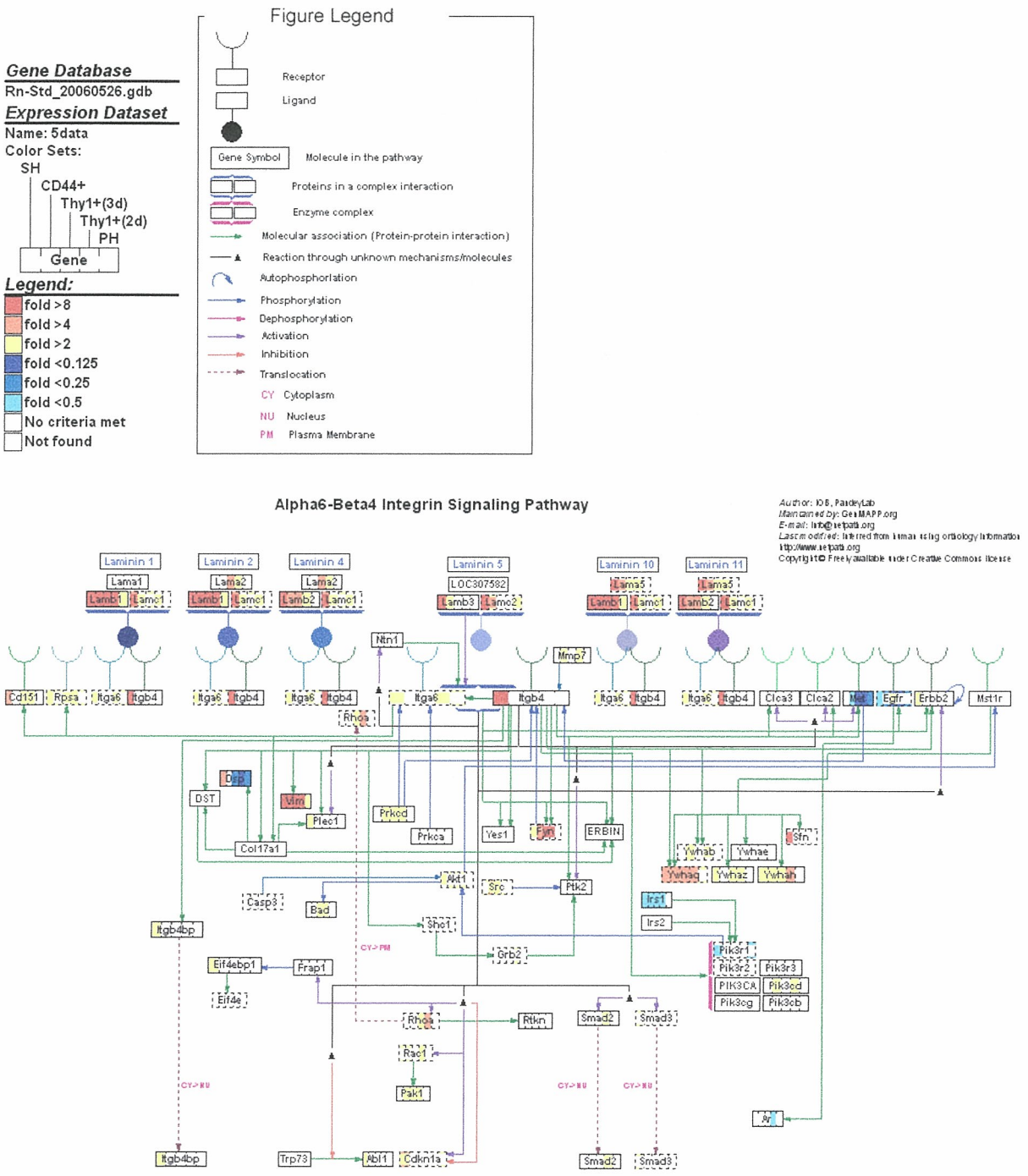
Gene Database
Rn-Std_20060526.gdb
Expression Dataset
Name: 5data
Color Sets:
SH
CD44+
Thy1+(3d)
Thy1+(2d)
PH
Gene
Legend:
fold >8
fold >4
fold >2
fold <0.125
fold <0.25
fold <0.5
No criteria met
Not found
Figure Legend
Receptor
Ligand
Gene Symbol
Molecule in the pathway
Proteins in a complex interaction
Enzyme complex
Molecular association (Protein-protein interaction)
Reaction through unknown mechanisms/molecules
Autophosphorlation
Phosphorylation
Dephosphorylation
Activation
Inhibition
Translocation
CY Cytoplasm
NU Nucleus
PM Plasma Membrane
Alpha6-Beta4 Integrin Signaling Pathway
Laminin 1
Laminin 2
Laminin 4
Laminin 5
Laminin 10
Laminin 11
Ntn1
Mmp7
Cd151
Rpsa
Itga6
Itgb4
Rhoa
Dpp
DST
Vim
Plec1
Col17a1
Prkcd
Prkca
Yes1
Fyn
ERBIN
Sfn
Ywhab
Ywhae
Ywhag
Ywhaz
Ywhah
Akt1
Src
Ptk2
Casp8
Bad
Shc1
Irs1
Irs2
Itgb4bp
Grb2
Pik3r1
Pik3r2
Pik3r3
PIK3CA
Pik3cd
Pik3cg
Pik3cb
Eif4ebp1
Frap1
Eif4e
Rtkn
Smad2
Smad3
Rac1
Pak1
Trp73
Abl1
Cdkn1a
CY->PM
CY->NU

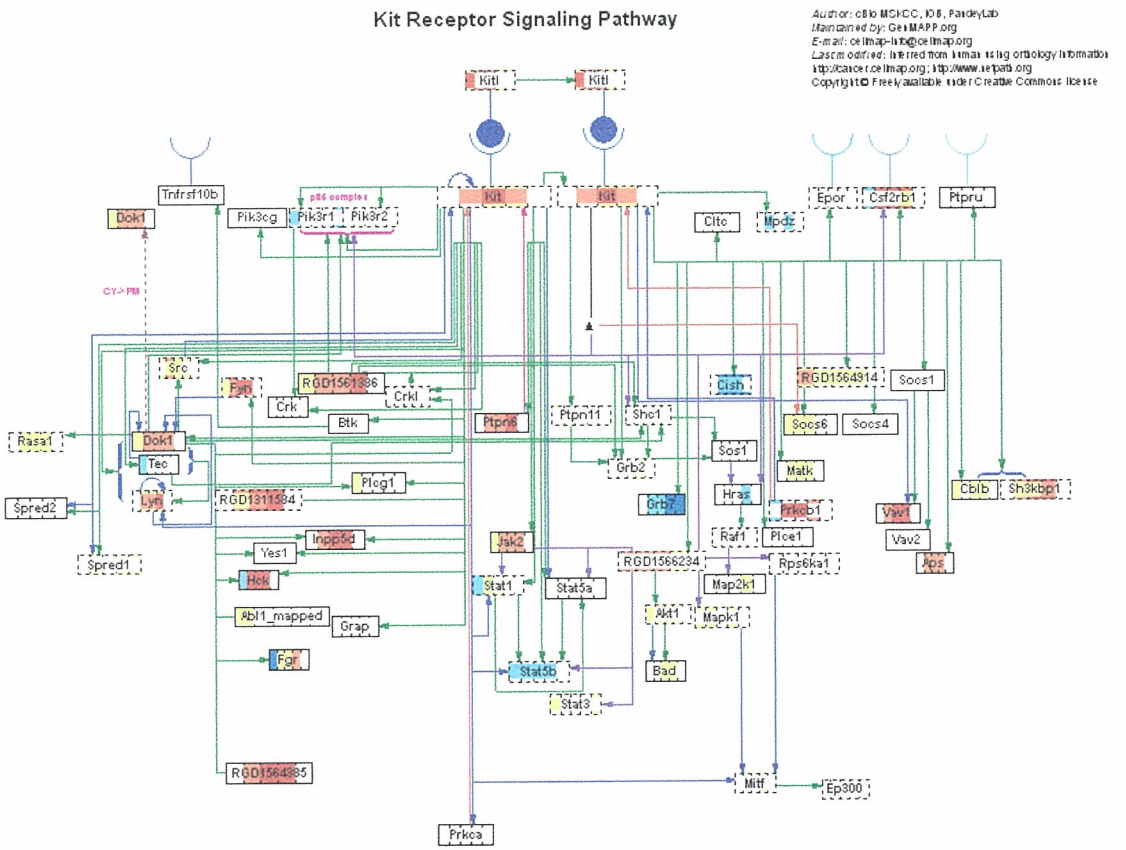
Kit Receptor Signaling Pathway
Kitl
Kit
Tnfrsf10b
Dok1
Pik3cg
Pik3r1
Pik3r2
Epor
Csf2rb1
Ptpru
Cltc
Hpdz
Src
Fyn
RGD1561886
Crk
Crkl
Btk
Ptpn6
Ptpn11
Shc1
Cish
RGD1564914
Socs1
Socs6
Socs4
Rasa1
Tec
Grb2
Sos1
Matk
Hras
Spred2
Lyn
RGD1311584
Plcg1
Grb7
Prkob1
Cblb
Sh3kbp1
Vav1
Vav2
Aps
Spred1
Inpp5d
Yes1
Jak2
Raf1
Plce1
Hck
RGD1566234
Rps6ka1
Stat1
Stat5a
Map2k1
Abl1_mapped
Grap
Akt1
Mapk1
Fgr
Stat5b
Bad
Stat3
RGD1564385
Mitf
Ep300
Prkca
TGF Beta Signaling Pathway
ligands:
RGD:1303119
TGFb
Tgfb1
Ltbp1
Inhba
Fst
Thbs1
Bmp4
Nog
Accessory receptors
Tgfbr3
Eng
Author: Nurit Gal and Manny Ramirez
Maintained by: Manny Ramirez
E-mail: genmapp@gladstone.ucsf.edu
Last modified: 12/10/03
Right-click here to see Notes
Copyright © 2002, Gladstone Institutes
Tgfbr2
Tgfbr1
Sara
Spp1
Sip1
Repressors
Rsmads
Fkbp1a
Bambi
Smad1
Smad5
Madh9
Madh2
Madh3
Co-smads
Madh4
Wnt1
Lif
Tnf
Catnb
Jak1
Mapk9
Runx2
Runx3
Lef1
Stat3
Jun
Tfe3
Fast
QAZ
Cofactors
Smad6
Madh7
Ifng
Tgfb1
Bmp4
Tnf
Stat1
Madh2
Smad1
Nfkb1
Egf
Mapk3
RAS
Cofactor
Co-Smads
R-Smads
P300
Crebbp
Tgif
SNO-N
SKI
Serpine1
Fos

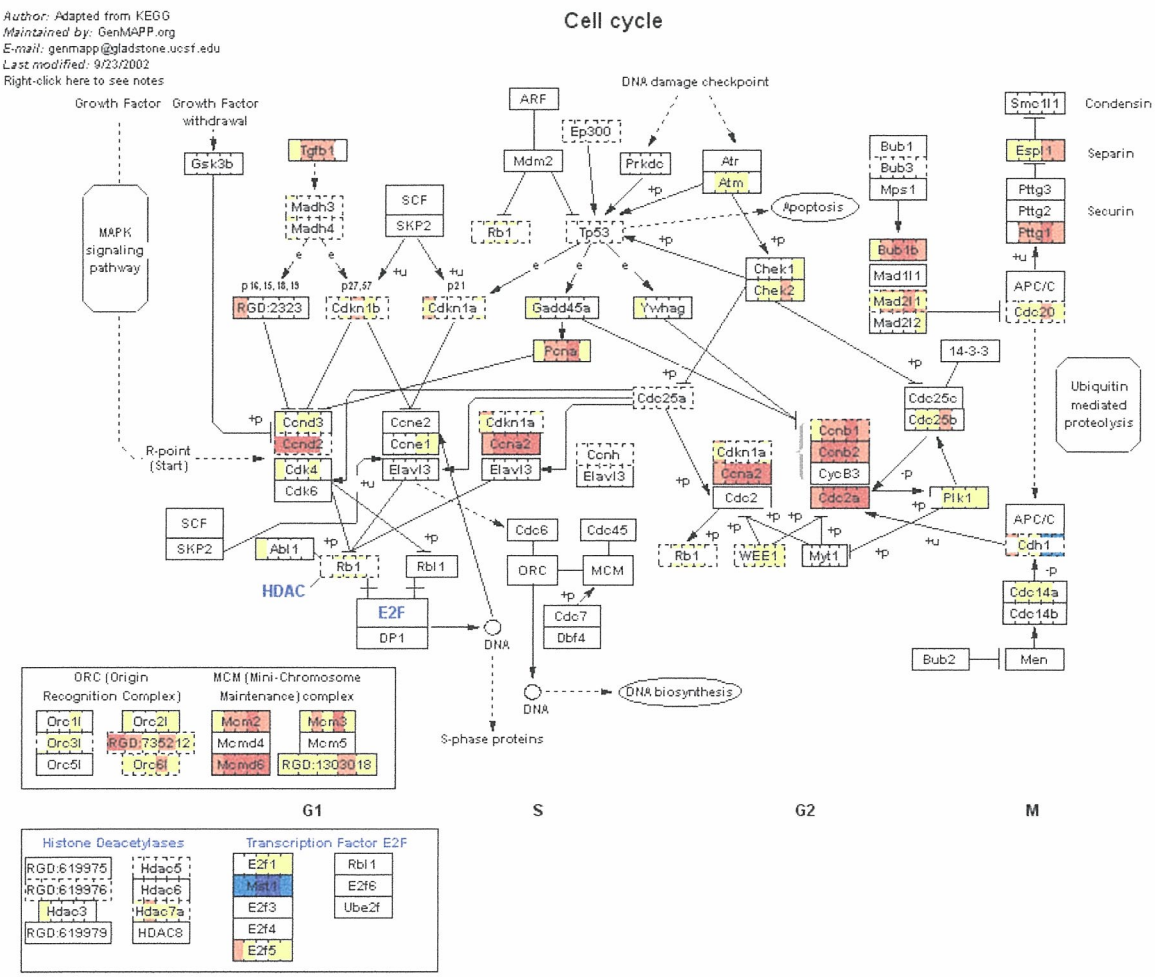
Author: Adapted from KEGG
Maintained by: GenMAPP.org
E-mail: genmapp@gladstone.ucsf.edu
Last modified: 9/23/2002
Right-click here to see notes
Cell cycle
Growth Factor
Growth Factor withdrawal
MAPK signaling pathway
Gsk3b
Tgfb1
Madh3
Madh4
SCF
SKP2
p16, 15, 18, 19
RGD:2323
p27,57
Cdkn1b
p21
Cdkn1a
ARF
Ep300
Mdm2
Rb1
DNA damage checkpoint
Prkdc
Atr
Atm
Tp53
Apoptosis
Gadd45a
Ywhag
Pcna
Chek1
Chek2
Bub1
Bub3
Mps1
Bub1b
Mad1l1
Mad2l1
Mad2l2
Smc1l1
Condensin
Espl1
Separin
Pttg3
Pttg2
Pttg1
Securin
APC/C
Cdc20
14-3-3
Cdc25c
Cdc25b
Ubiquitin mediated proteolysis
Cdc25a
R-point (Start)
Ccnd3
Ccnd2
Ccne2
Ccne1
Cdk4
Cdk6
Elavl3
Ccnh
Ccnb1
Ccnb2
CycB3
Cdc2a
Cdc2
Plk1
Abl1
Rb1
Rbl1
HDAC
E2F
DP1
DNA
Cdc6
Cdc45
ORC
MCM
Cdc7
Dbf4
WEE1
Myt1
Cdh1
Cdc14a
Cdc14b
Bub2
Men
DNA biosynthesis
S-phase proteins
ORC (Origin Recognition Complex)
Orc1l
Orc2l
Orc3l
RGD:735212
Orc5l
Orc6l
MCM (Mini-Chromosome Maintenance) complex
Mcm2
Mcm3
Mcmd4
Mcm5
Mcmd6
RGD:1303018
G1
S
G2
M
Histone Deacetylases
RGD:619975
RGD:619976
Hdac3
RGD:619979
Hdac5
Hdac6
Hdac7a
HDAC8
Transcription Factor E2F
E2f1
Mki1
E2f3
E2f4
E2f5
Rbl1
E2f6
Ube2f

研究成果の刊行に関する一覧表

雑誌

発表者氏名	論文タイトル名	発表誌名	巻号	ページ	出版年
吉川大和、 三高俊広	肝再生とラミニンα1鎖	**Surgery Frontier**	**13(2)**	**93-95**	2006
Nagaya M, Kubota S, Suzuki N, Akashi K, Mitaka T	Thermoreversible gelation polymer induces the emergence of hepatic stem cells in a partially injured rat liver	**Hepatology**	**43(5)**	**1053-1062**	2006
Kon J, Ooe H, Oshima H, Kikkawa Y, Mitaka T	Expression of CD44 in rat hepatic progenitor cells	**Journal of Hepatology**	**40(1)**	**90-98**	2006
Ooe H, Kon J, Miyamoto S, Oozone Y, Ninomiya S, Mitaka T	Cytochrome P450 expressions of cultured rat small hepatocytes after long-term cryopreservation	**Drug Metabolism and Disposition**	**34(10)**	**1667-1671**	2006
Nobuoka T, Mizuguchi T, Oshima H, Shibata T, Kimura Y, Mitaka T, Katsuramaki T, Hirata K	Portal blood flow regulates volume recovery of the rat liver after partial hepatectomy: Molecular evaluation	**European Surgical Research**	**38(6),**	**522-532**	2006

第49回　肝病態と細胞接着分子の新知見④

肝再生とラミニンα1鎖

1. 東京薬科大学薬学部病態生化学教室
2. 札幌医科大学がん研究所分子病理病態学部門

吉川　大和[1,2]・三高　俊広[2]
Yamato Kikkawa（講師）　*Toshihiro Mitaka*（教授）

はじめに

肝臓が他の臓器にみられない強い再生力をもっていることはよく知られている。肝臓の部分切除，薬物障害や疾患により，多くの肝細胞を一度に失うと，残存する肝細胞は同調して分裂し，肝再生が始まる。肝再生研究は，肝細胞を増殖させる肝細胞増殖因子（Hepatocyte growth factor：HGF）など増殖因子やその作用機序を中心に行われてきたが，肝再生では肝細胞の増殖に引き続き，細胞外マトリックスの再構成を伴った小葉構造の再構築が起こる[1)2)]。これまで細胞外マトリックスのひとつであるラミニンの肝臓における発現に関する報告は少なく，肝再生との関係も明らかではなかった。しかしながら，ラミニンを構成する鎖に特異的な抗体を用いて再評価を行ったところ，ラミニンα1鎖を含むラミニンが，肝再生時の組織再構成に関与することが示唆された。

ラミニンの構造とファミリー

ラミニンは，Ⅳ型コラーゲン，ニドゲン，パールカンとともに基底膜とよばれる組織支持構造体を形成し，細胞の基底膜への接着において中心的な役割を果たしている。ラミニンを構成する3本の鎖（図1-A）には，それぞれα鎖が5種類，β鎖が3種類，γ鎖が3種類あり，その組み合わせによって15種類のアイソフォームが存在することが報告されている（図1-B）。最近，ラミニンの命名法が1994年に続き改正された[3)4)]。3本の鎖の中でもα鎖は，ラミニンの生物活性にかかわる重要な鎖であり，そのC末端のLGドメインが最も重要な構造である。ラミニンアイソフォームの生体内における分布は組織特異的であり，関連する細胞の機能を制御している。詳しくは総説を参考にされたい[5)]。

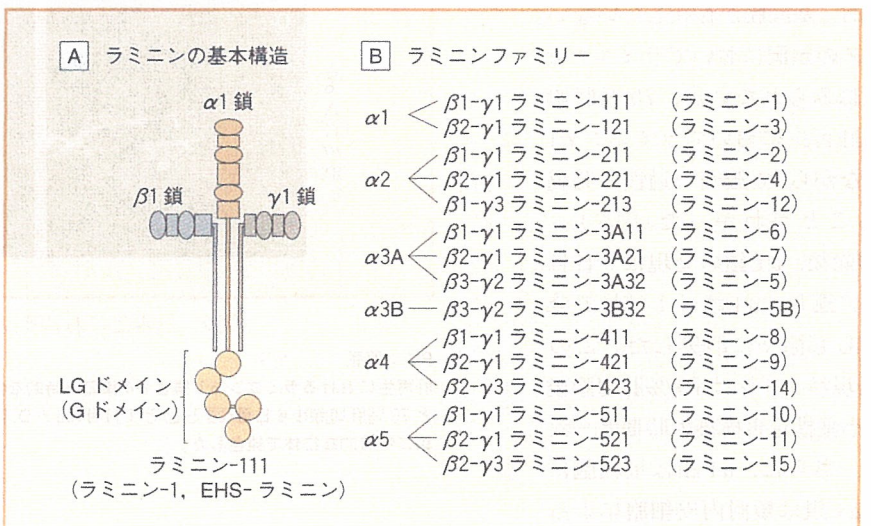

図1　ラミニンの構造とファミリー

A：ラミニン-111は，α1，β1，γ1鎖から構成され，マウスEHS（Engelbleth-Holm-Swarm）肉腫より最初に精製され，最も研究が進んでいるアイソフォームである。
B：生物活性を担うα鎖を中心に示した。各アイソフォームは，組織に特徴的な分布を示し，組織の機能に関与している（カッコ内は以前のアイソフォーム名）。

Surgery Frontier 13(2)：93-95，2006

肝臓におけるラミニンα鎖

ラミニンが局在する基底膜は，上皮細胞と結合組織または血管内皮細胞の間，筋線維の周囲などに存在している厚さ約 50 nm の薄い膜である。肝臓でも門脈や肝動脈，中心静脈，胆管の周囲などに基底膜の存在を確認することができる。ラミニンα鎖に特異的な抗体を用いて，正常マウスの肝臓を調べたところ，α5 鎖を含むラミニンが主要なアイソフォームであり，他の臓器における基底膜と同様に多様性をもつことが明らかになった(表 1)。また，ヒトの肝臓においても，α5 鎖を含むラミニンが主要なアイソフォームであることがわかってきている(未発表データ)。一方，肝臓の主要な部分を占める小葉の類洞において，肝細胞と類洞内皮細胞の間は Disse 腔とよばれ，例外的に基底膜が存在していない。正常マウスの類洞においてラミニンα鎖の発現はみられないが，70 %肝切除による肝再生においてラミニン α1 鎖と弱いながら α4 鎖が一過性に発現してくることがわかった(図 2)。70 %肝切除後，α1 鎖の発現は 6 日目でピークに達し，α4 鎖は 1 日目で発現しどちらも徐々に消失した。この α1 鎖の発現パターンは 70 %肝切除後に起こる小葉構造再構築の時期と一致していた。さらに，α1 鎖は星細胞によって，α4 鎖は類洞内皮細胞によって分泌されていた。

表 1　マウス肝臓におけるラミニンα鎖の発現

	ラミニンα鎖				
	α1	α2	α3	α4	α5
門脈	-	+/-	-	++	+++
胆管	-	-	++	-	+++
肝動脈	-	++	+	++	+++
類洞	+/-	-	-	+/-	-
中心静脈	-	-	-	+/-	+++
肝臓中皮	-	-	-	-	+++

(文献 6 より一部改変して引用)

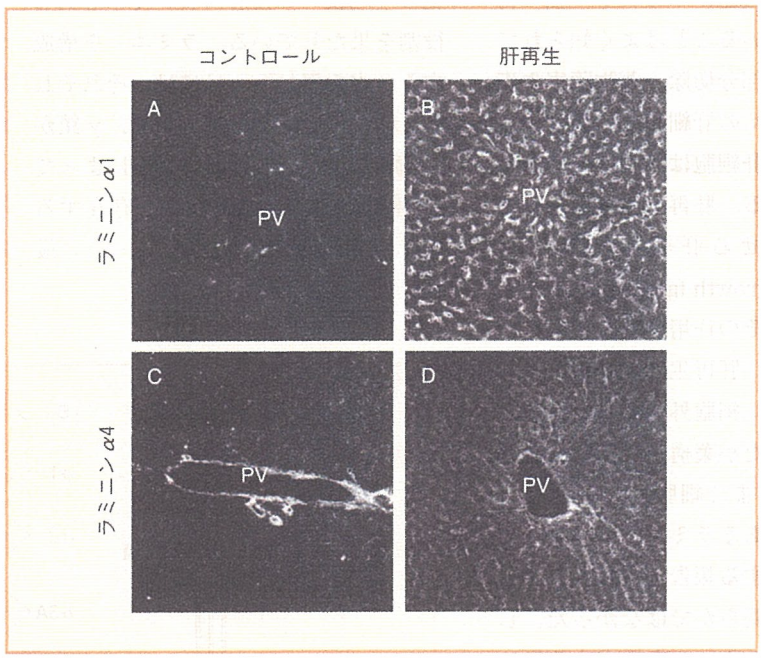

図 2　肝再生におけるラミニンα鎖

PV：門脈
肝再生におけるラミニン α1 鎖と α4 鎖の一時的な発現。コントロール(図 2-A，図 2-C)と 70 %肝切除後 6 日目(図 2-B)と 1 日目(図 2-D)の肝臓をそれぞれラミニン α1 鎖と α4 鎖に特異的な抗体で染色した。

(文献 6 より一部改変して引用)

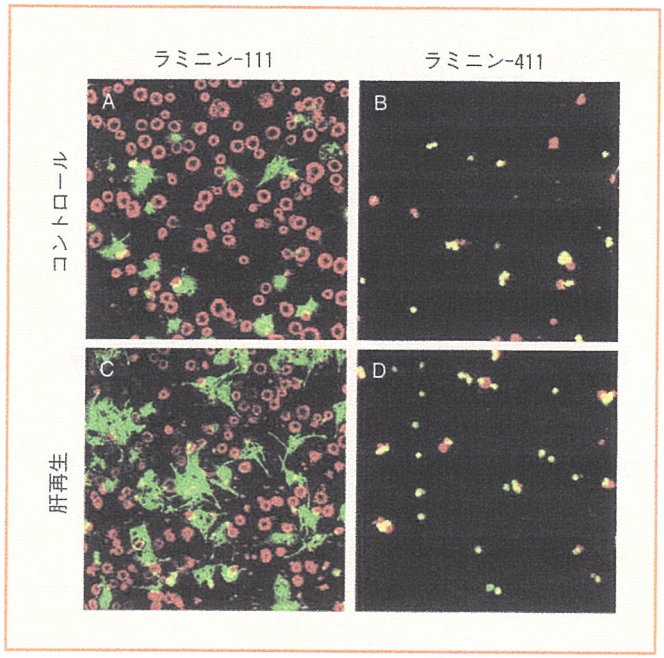

図3　肝細胞と類洞内皮細胞のラミニンに対する接着

α1鎖を含むラミニン-111（図2-A，図2-C）とα4鎖を含むラミニン-411（図2-B，図2-D）における肝細胞（赤）と類洞内皮細胞（緑）の形態。肝細胞は，ラミニン-111（α1鎖）に接着するだけで伸展しなかったが，類洞内皮細胞は伸展した（図2-A）。また，再生中の肝臓から単離された類洞内皮細胞はすでに活性化されているためか，正常肝臓より分離された細胞（図2-A）と比較して，運動に関与する仮足を伸ばすなど，より強く反応していた（図2-C）。

（文献6より一部改変して引用）

肝再生における α1鎖を含むラミニンの役割

肝再生において発現するα1鎖とα4鎖の役割を肝臓から単離した細胞によって検討を行ったところ，α4鎖を含むラミニンにはほとんどの細胞は接着しないが（図3），α1鎖を含むラミニンにはよく接着した。さらにα1鎖を含むラミニン上で類洞内皮細胞は，活性化されることがわかった。このことから，ラミニンα1鎖の一過性の発現は，小葉構造再構築における類洞内皮細胞の遊走などに関与していることが示唆された。

おわりに

肝臓疾患における問題点のひとつは，細胞外マトリックスの構成の乱れによって生じる組織の線維化である。肝再生は，増殖する肝細胞と細胞外マトリックスの再構成とのバランスの上に成り立ち，線維化することなく再生が行われる。肝再生におけるラミニンα1鎖の役割を解明することによって，肝臓の線維化メカニズムを解明する重要な手がかりが得られるのではないかと考えている。

文　献

1）Martinez-Hernandez A, Amenta PS：The extracellular matrix in hepatic regeneration. FASEB J 9：1401-1410, 1995
2）Michalopoulos GK, DeFrances MC：Liver regeneration. Science 276：60-66, 1997
3）Burgeson RE, Chiquet M, et al：A new nomenclature for the laminins. Matrix Biol 14：209-211, 1994
4）Aumailley M, Bruckner-Tuderman L, et al：A simplified laminin nomenclature. Matrix Biol 24：326-332, 2005
5）Miner JH, Yurchenco PD：Laminin functions in tissue morphogenesis. Annu Rev Cell Dev Biol 20：255-284, 2004
6）Kikkawa Y, Mochizuki Y, et al：Transient expression of laminin alpha 1 chain in regenerating murine liver：restricted localization of laminin chains and nidogen-1. Exp Cell Res 305：99-109, 2005

Thermoreversible Gelation Polymer Induces the Emergence of Hepatic Stem Cells in the Partially Injured Rat Liver

Masaki Nagaya,[1,4] Sunao Kubota,[2] Noboru Suzuki,[3] Katsuya Akashi,[1] and Toshihiro Mitaka[4]

Focal injury of the adult liver causes formation of granulomatous tissue and fibrosis. When thermoreversible gelation polymer (TGP) was applied to such defects of the rat liver, complete recovery of hepatic tissues was observed without granulation. We analyzed the mechanism of the regeneration. TGP is a chemically synthesized biocompatible polymer material whose sol-gel transition is reversible by changing the temperature. Cooled TGP was poured into a penetration lesion of the rat liver. Immunohistochemistry and polymerase chain reaction were carried out using tissues and cultured cells isolated from ductular structures. Immunocytochemical and ultrastructural analyses were also conducted. Seven days after TGP treatment, ductular reactions were observed around the wound and ductules elongated to the injured area. Cells in the structures were alpha-fetoprotein (AFP) positive, albumin$^+$, CK19$^+$, c-Kit$^+$, and Thy1$^+$. Hepatocyte-like cells possessing glycogen appeared around the tips of the ductules from day 9. The defect was completely replaced with hepatocytes by day 28. Cells isolated from the ductules expressed Musashi-1, c-Kit, Thy1, AFP, albumin, transferrin, connexin 43, and CK19. When the cultured cells were covered by TGP, they rapidly proliferated to form colonies, whereas without TGP cells gradually died. Morphologically and ultrastructurally the cells were similar to hepatocytes. They expressed not only albumin and transferrin but TAT, CYP2E1, and CCAAT/enhancer binding protein α. Some cells formed bile canaliculus-like structures. In conclusion, TGP may trigger the initiation of hepatic stem cells in biliary ductules, and stem cell activation may occur even in the regeneration of the normal liver. (HEPATOLOGY 2006;43:1053-1062.)

The mechanisms of regeneration in focal liver injury are not well understood. We found that the defect made by focal injury was usually replaced by granulomatous tissue. When we used thermoreversible gelation polymer (TGP) as a sealing material for the injury, efficient regeneration occurred without any granulation.[1] TGP is a chemically synthesized biocompatible polymer material.[2] It is soluble below a lower critical solution temperature (LCST) and becomes solid above the LCST. When soluble TGP is applied, it can infiltrate into any part. Thereafter, it immediately changes into gel at body temperature and causes complete sealing of the defect, leading to efficient regeneration of the liver.[1] However, the mechanisms of the regeneration with TGP treatment have largely remained unknown.

The liver appears to have three distinct mechanisms of regeneration in response to loss of hepatocytes: (1) Mature hepatocyte (MH)s proliferate in case of partial hepatectomy and centrolobular injury by hepatotoxins.[3-5] Surviving hepatocytes immediately proliferate and restore the original mass[4]; (2) When the proliferation of hepatocytes is inhibited by some toxins such as 2-acetylaminofluorene, hepatic growth stimulation results in emergent ductules, and the cells in the ductules gradually migrate into the hepatic parenchyma.[3-5] "Oval cells" or "ductular hepatocytes" are involved in the ductular reaction in rodents.[5,6] These cells may be derived from putative stem cells and may differentiate into hepatocytes; (3) Bone

Abbreviations: TGP, thermoreversible gelation polymer; LCST, lower critical solution temperature; MH, mature hepatocyte; NIH, National Institutes of Health; HE, hematoxylin-eosin; PAS, periodic acid-Schiff; TEM, transmission electron microscopy; AFP, alpha-fetoprotein; CK19, cytokeratin 19; PCNA, proliferating cell nuclear antigen; C/EBPα, CCAAT/enhancer binding protein α; MRP2, multidrug-resistance associated protein 2; BEC, bile epithelial cell; BDL, common-bile-duct ligation; NT, no treatment; CG, collagen gel; FG, fibrin glue; POD, post operative day; BC, bile canaliculi.

From the [1]Department of Emergency and Critical Care Medicine; the [2]Department of General Surgery; the [3]Department of Immunology and Medicine; St. Marianna University, School of Medicine, Kawasaki, and the [4]Department of Pathophysiology, Cancer Research Institute, Sapporo Medical University School of Medicine, Sapporo, Japan.

Received October 14, 2005; accepted February 13, 2006.

Supported by Grants-in-Aid from the Ministry of Education, Culture, Sports, Science and Technology of Japan (15790708 to M.N. and 14370393, 17390353 to T.M.) and the Marumo Fund (to M.N).

Address reprint requests to: Masaki Nagaya, M.D., Ph.D., Department of Emergency and Critical Care Medicine, St. Marianna University, School of Medicine, Kawasaki 261-8511, Japan. E-mail: m2nagaya@marianna-u.ac.jp; fax: (81) 44-979-1522.

Published online in Wiley InterScience (www.interscience.wiley.com).

DOI 10.1002/hep.21153

Potential conflict of interest: Nothing to report.

marrow–derived cells may participate in hepatic regeneration.[4,5,7]

Here we report that, in the hepatic regeneration of focal injury by TGP, ductular reactions are initially induced, and hepatic stem cells involved in the ductules may differentiate into hepatocytes. In addition, cells isolated from the ductules induced by TGP treatment can rapidly proliferate and differentiate into hepatic cells when the cells are covered by TGP. Thus, hepatic stem cells may participate in hepatic regeneration even when no hepatotoxins are involved in the injury.

Materials and Methods

Animals and Surgery. Adult male Fisher 344 rats were obtained from Charles River (Atsugi, Kanagawa, Japan). All animals received humane care, and the experimental protocol was approved by the Committees of Laboratory Animals of St. Marianna and Sapporo Medical Universities and was in accordance with National Institutes of Health (NIH) guidelines. The total number of sacrificed rats was over 150, and at least five animals/point were examined. A penetrating, 4-mm-diameter defect was made in left middle lobe of the liver at a distance of 10 mm from lobular edges. The rats were then randomly assigned into three groups: penetration alone (control), penetration filled with fibrin glue (FG, Kaketsuken, Kumamoto, Japan), and penetration filled with TGP (TGP, Mebiol, Tokyo, Japan). FG and TGP (0.5 mL) were poured into the penetrated site.

Preparation of TGP. N-isopropylacrilamide, Eastman Kodak, New York, NY) was recrystallized from acetone and copolymerized with N-acryloxysuccinimide (Kokusan Chemical, Tokyo, Japan) to provide an activated form of Poly- N-isopropylacrilamide. Polymerization was carried out in $CHCl_3$, using azobisisobutyronitrile as the initiator. The activated copolymer was precipitated with diethylether and recovered. Then the copolymer and diamino-polyethylene glycol (Kawaken Fine Chemicals, Tokyo, Japan) were dissolved in $CHCl_3$ and reacted. The byproduct, N-hydroxylsuccinimide, was removed and the remaining solution was lyophilized to yield TGP. Saline was added to the TGP to adjust it to 5.5 % (wt/wt). The LCST was approximately 20°C[2], and toxicity of TGP was not observed.[1]

Histology. Liver tissues were obtained from the injured lobe, and other lobes were used as a control. Liver specimen (diameter 10 mm) surrounding the injured region was enucleated in a cylindrical shape. The specimen was cut in half, and both paraffin and frozen samples were prepared. The ventral halves of the specimens were fixed with 4% paraformaldehyde in phosphate-buffered saline and embedded in paraffin. To evaluate the size of the injury lesion, the area of fibrosis in hematoxylin-eosin (HE)-stained sections was measured and analyzed using a light microscope equipped with a CCD camera and AxioVision AC Rel. 4.1 software (Carl Zeiss, Jena, Germany). In addition, to evaluate the hepatic lobule size, the distance between portal veins was measured. The proximal portion less than 3 mm from the injured site and the distal portion farther than 5 mm from the injured site were evaluated. Periodic acid-Schiff (PAS)-staining was performed to examine the production of glycogen. Diastase was applied to test whether PAS-positive materials were glycogen.[8] The procedure used for transmission electron microscopy (TEM) was previously described.[9]

Immunostaining. Antibodies to c-Kit (Santa Cruz, CA), Thy1 (Pharmingen, Hamburg, Germany), α-fetoprotein (AFP; Dako Cytomation, Kyoto, Japan), albumin (Dako Cytomation), cytokeratin 19 (CK19; Novocastra Laboratories, Newcastle, UK and a gift of Dr. A. Miyajima, Tokyo University, Japan), proliferating cell nuclear antigen (PCNA; Dako Cytomation), Ki67 (Pharmingen), CCAAT/enhancer binding protein α (C/EBP α; Santa Cruz), and multidrug-resistance associated protein 2 (MRP2; Alexis Biochemichals, San Diego, CA) were used. The methods used for immunohistochemistry and immunocytochemistry were previously described.[9] 3, 3′-Diaminobenzidine and BCIP/NBT (Dako Cytomation) were used as a substrate for colorization. $Alexa^{488}$-conjugated and $Alexa^{594}$-conjugated antibodies (Molecular Probes, Eugene, OR) were used as secondary antibodies.

CK19 and Albumin Double-Positive Cells in the Ductules. Immunohistochemistry for CK19/albumin was carried out. The number of $CK19^+$/$albumin^+$ cells in the ductules in the upper right quadrant area was counted, which included part of the injured areas. Simultaneously, we measured the size of the area by using NIH image software.

Isolation and Culture of Ductular Cells. Intrahepatic biliary epithelial cell (BEC)s were separated from normal, common-bile-duct-ligated (BDL), and TGP-treated rat livers. To isolate the cells from the injury lesion, two-step liver perfusion[9] was initially carried out 1 week after operation. The tissue was enucleated in a cylindrical shape (diameter 10 mm) surrounding the injured site and transferred into a Petri dish. After hepatocytes were removed, the remnant tissues were collected, transferred into a flask, and then treated with collagenase, dispase (Godo Shyusei, Tokyo, Japan) and hyaluronidase (Sigma, St Louis, MO) for 30 minutes. The digested tissues were suspended in Dulbecco's modified Eagle's medium and centrifuged at 150*g* for 10 minutes. The pellet was resuspended in the medium, filtered

Table 1. Sequences of PCR Primers

Primer	Sequence (5′-3′)	Anneling Temperature (°C)	PCR Product (bp)
GAPDH	CCATCACCATCTTCCAGGAG	60	576
	CCTGCTCACCACCTTCTTG		
Musashi-1	ATGCCATGCTGATGTTCGAC	60	255
	ACCCTGGGTAACCTAACATG		
c-Kit	CATCATGGAAGATGACGAG	60	281
	CAAATGTGTACACGCAGCTG		
Thy1	ACAAGCTCCAATAAAACTATCAATGTGAT	60	84
	GGAAGTGTTTTGAACCAGCAGG		
AFP	TGAAATTTGCCACGAGACGG	60	272
	TGTCATACTGAGCGGCTAAG		
Albumin	GACAAGTTATGCGCCATTCC	60	288
	ACTGGGTCAGAACCTCATTG		
Transferrin	TGTCTGAGCATGAGAACACC	60	299
	GTTCAGCTGGAAGTCTGTTC		
TAT	TACTCAGTTCTGCTGGAGCC	60	471
	GCAAAGTCTCTAGAGAGGCC		
CYP2E1	AGCACAACTCTGAGATATGG	60	365
	ATAGTCACTGTACTTGAACT		
CYP3A1	CAGCTCTCACACTGGAAACCTGGG	60	689
	CTCATATATTTGGGGTGAGGAATGG		
CX43	GGAAAGTACCAAACAGCAGC	60	348
	AGGACTTGTCATAGCAGACG		
CK19	ATGACTTCCTATAGCTATCG	60	340
	CACCTCCAGCTCGCCATTAG		
CX18	GGACCTCAGCAAGATCATGGC	60	515
	CCACGATCTTACGGGTAGTTG		
HNF3α	TTCGGAGTTGAAGTCTCCAG	60	218
	CATATGCCTTGAAGTCCAGC		
HNF4	TCTACAGAGCATTACCTGGC	60	614
	TGAGGGGAAGATGAAGACGG		
C/EBPα	TTCCAGATCGCACACTGCCC	60	404
	TGACCAAGGAGCTCTCAGGC		
HNF6	GACAAATGGCAGGACGAGGG	60	681
	AGCGTACTGGTTTAGGTGCC		

NOTE. GAPDH was used as an internal control.

through 70-μm nylon mesh, and small cell aggregates on the mesh were selectively picked up using a pipette. The cell aggregates were suspended in Dulbecco's modified Eagle's medium supplemented with 10% fetal bovine serum, 10 mmol/L nicotinamide, 1 mmol/L ascorbic acid 2-phosphate, 10 ng/mL epidermal growth factor (Collaborative Research, Lexington, MA), 10^{-7} mol/L dexamethasone, 0.5 μg/mL insulin, and antibiotics. Then 200 cell aggregates were plated on a 35-mm dish. Seven days after plating, the dishes were randomly divided into 3 groups: no treatment (NT), cells overlaid with collagen gel (CG), and cells overlaid with TGP gel (TGP). The specific gravity of both collagen gel and TGP was adjusted to 1.06 mg/mL.

Polymerase Chain Reaction. Total RNA was isolated from ductules and cultured cells, and reverse transcriptase-polymerase chain reaction was conducted as previously described.[10] Primers are listed in Table 1.

Colony Counts. We measured colony number and size using a phase-contrast microscope (Olympus Optical, Tokyo, Japan) equipped with a CCD camera.

Statistics Analysis. Data are shown as mean ± SEM. ANOVA and Fisher's protected least significant difference test were used, and a P value $<.05$ was considered significant.

Results

Histology of the Liver Injury. At day 28, we macroscopically observed complete recovery of liver tissue in the TGP group, whereas in livers of both the control and FG groups fibrosis was apparent in the lesions. As shown in Fig. 1, in the control group, the hole was left open, and exudates accumulated at postoperative day 3 (POD 3, Fig. 1B). Thereafter, inflammatory and fibroblastic cells gradually gathered and formed granulomatous tissue at POD 7, which became larger and more prominent at POD 14 (Fig. 1C) and POD 28 (Fig. 1D). In the FG group, inflammatory cells and fibroblastic cells invaded the FG at POD 3 (Fig. 1F). The FG remained in the center of the lesion and fibrosis was observed at the periphery of the defect at POD 14 (Fig. 1G). Granuloma-

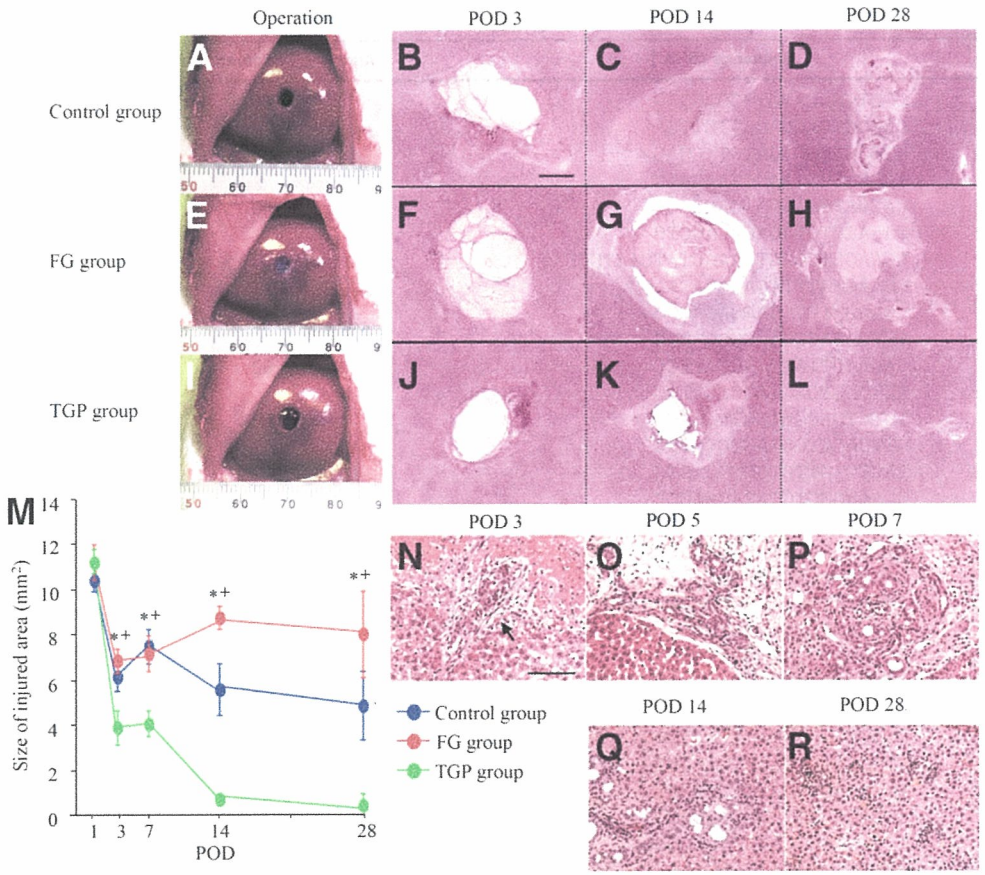

Fig. 1. Histological analysis of the partially injured rat liver filled with TGP. A penetrating wound was made in the left middle lobe (A). The hole was left open (control group). Exudates and coagulation accumulated in the injury site at POD 3 (B). Inflammatory cells and fibroblasts gradually formed granulomatous tissue, and scar formation then became evident at POD 14 (C) and POD 28 (D). Fibrin gel was poured into the lesion (E; FG group). The inflammation was evident inside and around the gel at POD 3 (F). FG changed to granuloma and the size of the injured area was enlarged at POD 14 (G). Hepatic regeneration did not occur at POD 28 (H). The hole was filled with TGP (I; TGP group). A thin layer of connective tissues surrounding TGP was observed at POD 3. The area of TGP became small and the injured area gradually shrank at POD 14 (K). Most of the injured area was replaced with hepatic cells, and only a small amount of fibrosis remained at POD 28 (L). B-D, F-H, and J-L show HE staining at the same magnification. Scale bar, 1 mm. Change of the size of the injured area after operation in each group (M). Bars show mean ± SEM of five samples. TGP versus *Control and +FG, $P < .05$. Histological appearance of the liver tissues treated with TGP: Ductular reactions (an arrow) emerged at POD 3 (N). They elongated from the portal areas located at the boundary between intact hepatocytes and dead cells. The ductules extend toward the injured area at POD 5 (O). The cells in ductular reactions became columnar-like structures at POD 7 (P). The hepatocyte-like cells increased around the ductules at POD 14 (Q). On POD 28, most ductules have disappeared and the lesion is almost completely replaced with hepatocytes (R). N-R are the same magnification. Scale bar, 100 μm. TGF, thermoreversible gelation polymer; POD, postoperative day; FG, fibrin glue; HE, hematoxylin-eosin.

tous tissue was observed even at POD 28 and no replacement of hepatocytes was observed (Fig. 1H). In the TGP group, the TGP-occupied area was observed as a vacant area (Fig. 1J) that gradually shrank with time (Figs. 1J-L). Between the vacant area and intact hepatocytes, a relatively narrow area of tissue consisting of epithelial and fibroblastic cells, some inflammatory cells, and fibrosis were observed at POD 14 (Fig. 1K). Although a small amount of fibrosis remained, the lesion was almost completely replaced by hepatocytes at POD 28 (Fig. 1L). As shown in Fig. 1M, the size of the injured area dramatically decreased in the TGP group, whereas it did not change in the FG group and decreased by half in the control group. To examine whether remnant MHs surrounding the injured area participated the regeneration, we measured the sizes of neighboring lobules. Lobules not only proximal but also distal to the injury were not enlarged during regeneration (data not shown).

As shown in Fig. 1N, ductular reactions were first observed at POD 3 in the TGP group. The ductules might have originated from the presumptive area of portal triads and elongated toward the center of the injury. The length and the number of the ductules gradually increased until POD 7 (Fig. 1O-P). Compared with normal BECs, the cells in the ductules had relatively large cytoplasms and round nuclei, although both were smaller than those in

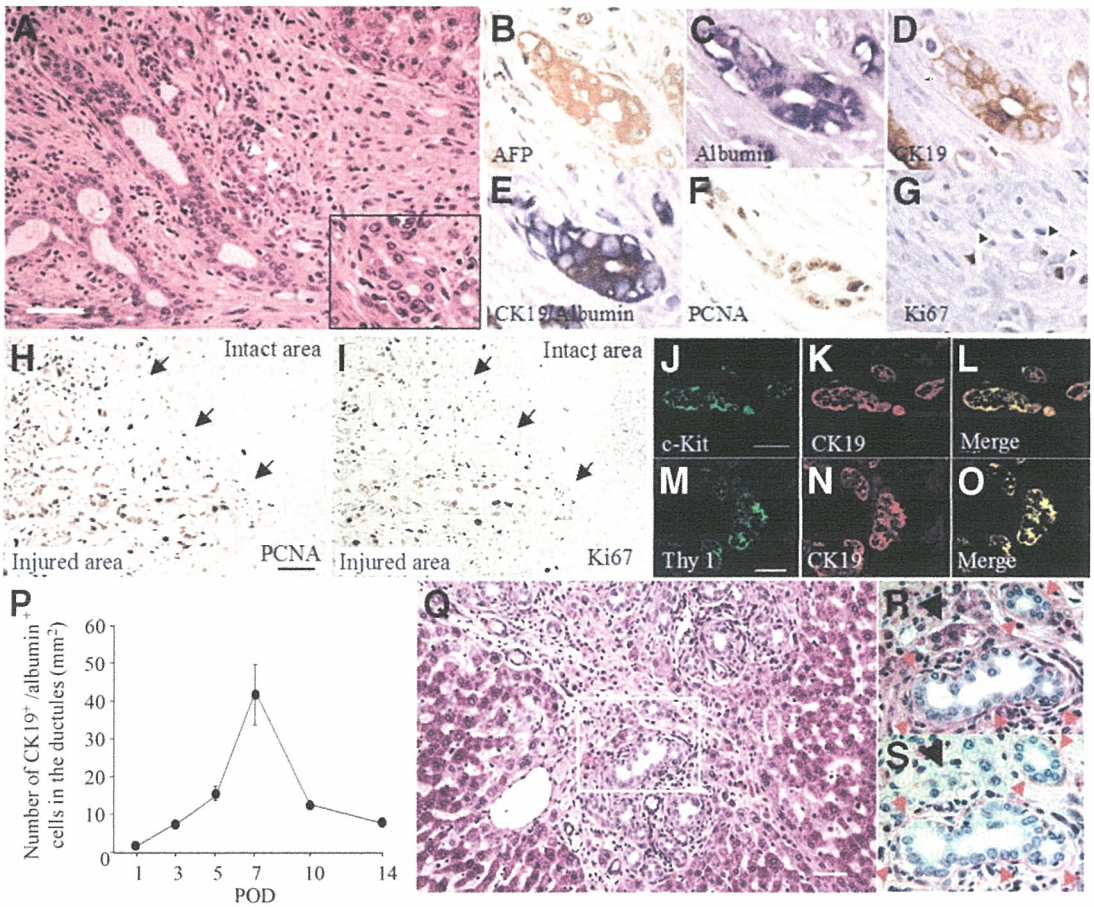

Fig. 2. Characterization of the cells in ductular reactions induced by TGP. Serial sections of the liver tissues were prepared and immunohistochemistry was carried out at POD7. HE staining (A): inset shows the enlargement of the location indicated by white arrowheads. Scale bar, 100 μm. Immunohistochemistry for AFP (B), albumin(C), CK19 (D), PCNA (F, H), and Ki67 (G, I). (E) Double staining of CK19 and albumin. Arrowheads in F and G show Ki67$^+$ nuclei. Immunohistochemistry for PCNA (H) and Ki67 (I) shows that relatively few adjacent hepatocytes (intact area) have positive nuclei at POD 7. Arrows in H and I show the boundary between the injured area and intact area. Scale bar, 100 μm. Fluorescent double immunohistochemistry for c-Kit/CK19 (J-L) and Thy1/CK19 (M-O) of the cells in ductular reactions at POD 7. Scale bar, 100 μm. (P) The number of CK19$^+$/albumin$^+$ cells in the ductules in the upper right quadrant area was counted, which included part of the injured areas. Simultaneously, we measured the size of the area (mm^2) by using NIH image software. Based on the above measurements, we calculated cells/mm^2. The peak of the number was observed at POD 7. We used five rats at each time point, and one slide per rat was prepared for the measurement. The results are shown as mean $\pm$ SEM of five rats. PAS-staining of the cells in ductular reactions at POD 9 (Q-S). (R and S) Enlargement of the square shown in Q. The section was pretreated with diastase before PAS-staining (S). Pinkish granules are observed in the cytoplasm of hepatocyte-like cells around ductules (R, black arrowhead), and basement membrane (positive lines) is surrounding the ductules (red arrows). The pinkish granules in hepatocyte-like cells disappeared after diastase treatment (S, black arrowhead), whereas the linear staining remained around the ductules (S, red arrows). Scale bar, 100 μm. TGF, thermoreversible gelation polymer; POD, postoperative day; FG, fibrin glue; HE, hematoxylin-eosin; AFP, alpha-fetoprotein; PCNA, proliferating cell nuclear antigen; SEM, scanning electron microscopy; PAS, peroidic acid-Schiff.

MHs. The cells in ductules changed their configuration from rectangular to columnar, and hepatocyte-like cells appeared surrounding the ductules (Fig. 1P-Q). At POD 28, the injury lesion was replaced by hepatocytes, and most ductules disappeared. No ductular proliferation was detected in either the control or FG group. Characterization of the cells in ductular reactions was carried out by immunostaining. At POD 7, most cells had CK19, albumin, and AFP (Fig. 2B-E). In addition, 68% and 72% of CK19$^+$ cells in the ductules were c-Kit$^+$ and Thy1$^+$, respectively (Fig. 2J-O). To examine the growth activity of the cells, immunostaining for PCNA and Ki67 was performed. As shown in Fig. 2F-I, many cells in ductular reactions possessed PCNA$^+$ or Ki67$^+$ nuclei, whereas relatively few MHs surrounding the ductular reactions had positive nuclei. The number of CK19$^+$/albumin$^+$ cells in the ductules was counted and the peak was observed at POD 7 (Fig. 2P). The largest numbers of c-Kit$^+$, Thy1$^+$, AFP$^+$, PCNA$^+$ and Ki67$^+$ cells were also observed at POD 7 (data not shown).

As shown in Fig. 2Q-R, hepatocyte-like cells surrounding the ductules appeared at approximately POD 9. To

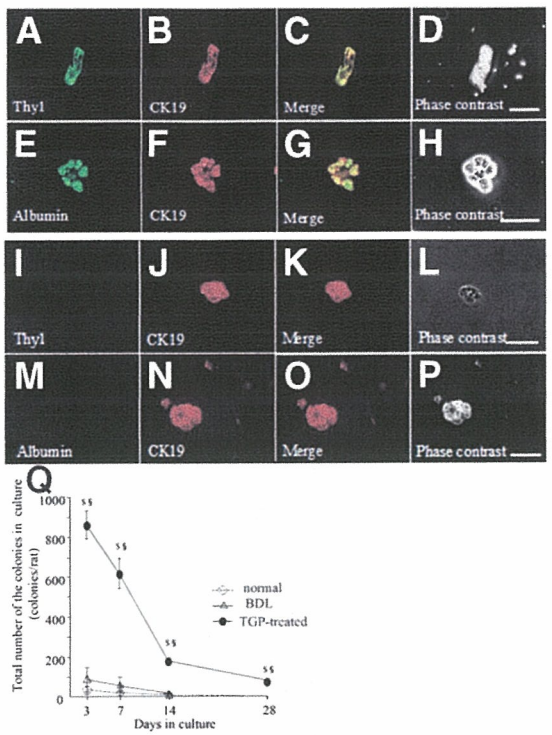

Fig. 3. Characterization of isolation and culture of the ductular cells from a TGP-treated rat liver. Double immunostaining of the cells for Thy1/CK19 (A-C and I-K) and albumin/CK19 (E-G and M-O) was conducted. (D, H, L, and P) Phase-contrast photos of the corresponding cells. Approximately 72% of the isolated cells were Thy1$^+$. CK19$^+$ cells from a normal rat liver were Thy1$^-$ (I) and albumin$^-$ (M). Scale bars, 100 μm. (Q) Total number of colonies per rat. The cells were isolated from normal rats (normal), rats with BDL, and rats treated with TGP (TGP-treated). The ordinate shows the total number of colonies per rat. The points show mean $\pm$ SEM of five independent experiments using five rats. TGP versus normal[$] and BDL[§], $P < .05$. TGF, thermoreversible gelation polymer; BDL, bile duct ligated.

examine whether the cells were hepatocytes, PAS staining was performed (Fig. 2R-S). Reddish granules in cytoplasm (Fig. 2R) were observed, and the materials were digested by diastase (Fig. 2S). Conversely, basement membrane surrounding the ductules was not digested. The results proved that the hepatocyte-like cells possessed glycogen in their cytoplasm and were hepatocytes.

Isolation and Culture of Cells in TGP-Induced Ductules. Cells in ductules were isolated from the TGP-treated rat livers and formed small aggregates. To characterize the cells, immunocytochemistry for CK19 and Thy1 was conducted. We found that 89% and 84% of the attached cells were CK19$^+$ and Thy1$^+$, respectively (Fig. 3A-D). Moreover, most CK19$^+$ cells expressed both albumin (Fig. 3E-H) and c-Kit (data not shown). When the same manipulation was performed for rats of the control and FG groups, although few cells were isolated, all cells died in early culture. Therefore, we used BECs from normal and BDL rats as controls. Although all CK19$^+$ BECs isolated from normal and BDL rats survived more than 2 weeks, they did not express Thy1 or albumin (Fig. 3I-P). After plating, the cells from the TGP-treated rats started to grow from day 3 and formed colonies. Colonies sometimes fused and formed a large colony. The number of colonies decreased with time in culture but was significantly higher in the TGP-treated than in both the normal and BDL rats. As shown in Fig. 3Q, the number of ductules from a TGP-treated rat was clearly larger than those from both normal and BDL rats. The cells from the ductules of the TGP-treated rat could survive for more than 60 days. Hepatic cells did not contaminate this culture.

Effects of TGP on the Cells From Ductules. To examine whether TGP could induce hepatic differentiation of the cultured ductular cells, the cells were overlaid with TGP gel from day 7. The cells extensively proliferated, and the colonies became large (Fig. 4D). To exclude the possibility that any gel overlay could induce the differentiation, collagen gel was used as a control. The number of the surviving colonies in all cultures from the 3 groups rapidly decreased with time in culture (Fig. 4E). However, after TGP overlay, the degree of the decrease was suppressed. The slight decrease in the number of colonies in TGP was due to the fusion of neighboring colonies and, therefore, each colony became a large one. Approximately 20 colonies/dish survived in TGP and continued proliferating with time in culture (Fig. 4F). More than 1 month later, cells with large cytoplasm appeared around the periphery of some colonies (Figs. 4G-H). The cells expressed not only albumin but also C/EBPα, which is expressed in differentiated hepatocytes (Fig. 4I). As shown in Fig. 4J, translucent belts were sometimes observed between large cells. These cells expressed albumin (Fig. 4L), and MRP2 was immunocytochemically stained along the structure (Fig. 4K). Therefore, the structures might have been bile canaliculi (BC). Most colonies in NT and CG disappeared by day 42.

To observe the cultured cell ultrastructures, perpendicular sections were prepared using the semithin sections of the samples for TEM. As shown in Fig. 5A, a one- or two-cell layer of columnar cells was arranged on connective tissues, and the cells were larger than 10 $\times$ 10 μm, and thus perhaps larger than BEC and smaller than MH. Transversal sections also showed that the colonies consisted of relatively large cells (Fig. 5B). Although the existence of peroxisomes was not proved, the cells possessed many organella such as mitochondria and rough endoplasmic reticulum. In addition, BC-like structures with many microvilli were observed between the cells (Fig. 5C).

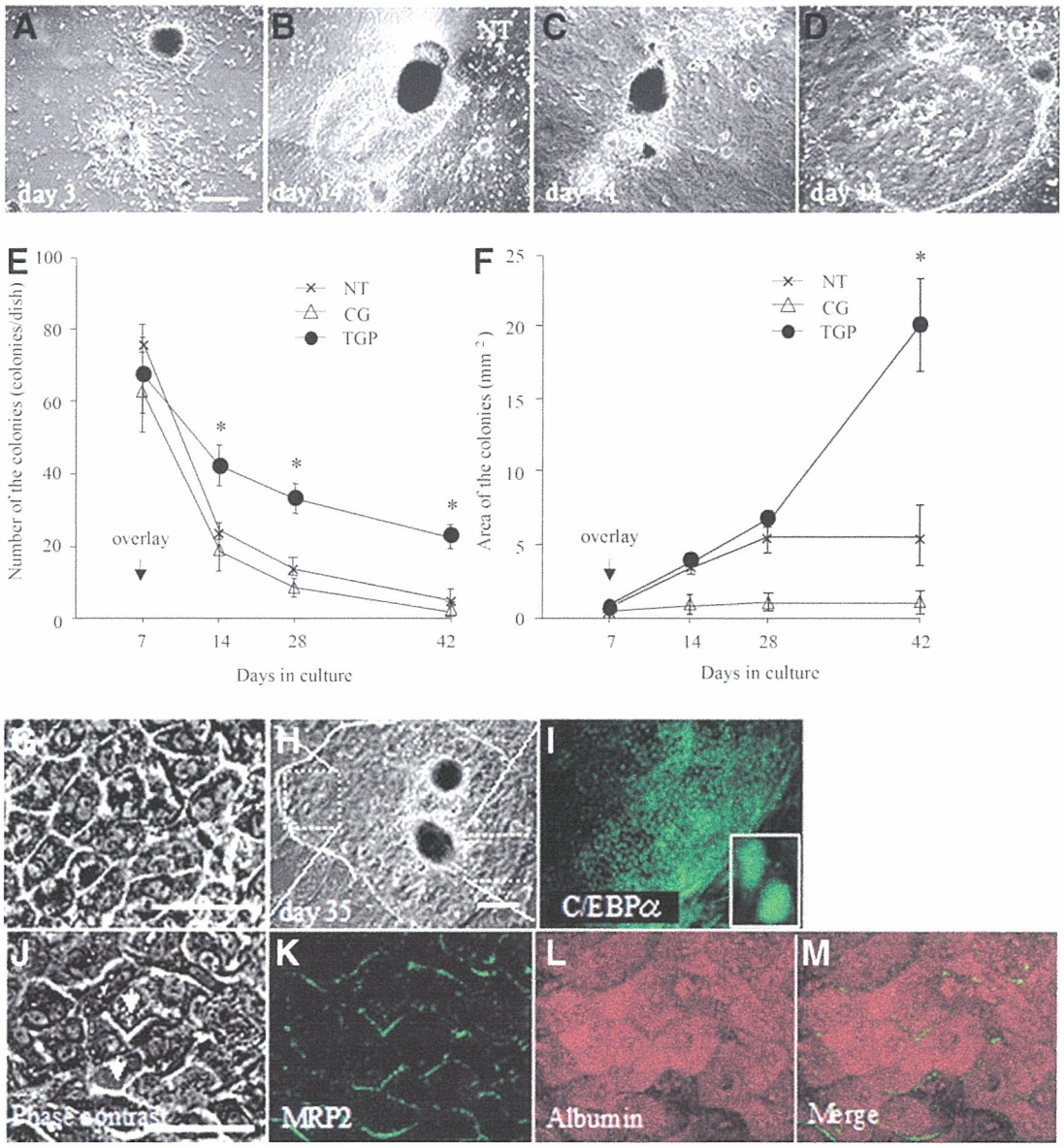

Fig. 4. Culture of the cells isolated from a rat liver treated with TGP. The isolated cells were plated on dishes. The cells initially formed small aggregates and expanded to form colonies with time in culture. Seven days after plating, the cultures were randomly assigned into three groups: Cells were overlaid with nothing (NT), 1 mL collagen gel (CG), and 1 mL TGP gel (TGP). The cells proliferated to form colonies (A), and the colonies continued expanding (B). The cells under CG marginally grew from aggregates (C). The cells under TGP showed rapid expansion to form large colonies (D). The number (E) and the size (F) of the colonies in the cultures were measured. Bars show mean ± SEM of five independent experiments. The number of the colonies at day 3 in each group (NT, CG, and TGP) was 170.8 ± 5.3, 161.6 ± 10.4, and 151.6 ± 7.3, respectively. The area of the colonies at day 3 in each group (NT, CG, and TGP) was 0.26 ± 0.06, 0.21 ± 0.03, and 0.23 ± 0.04 mm^2, respectively. TGP versus *both groups, $P < .05$. Characterization of the cells overlaid with TGP at day 35 (G-M). (G) Enlargement of the location in H indicated by the dotted rectangle. Cells with relatively large cytoplasm are mainly observed in peripheral portions of expanding colonies. Many cells have two nuclei. Scale bar in G, 100 μm. Scale bar in H, 1 mm. Fluorescent immunocytochemistry for C/EBPα (I), MRP2 (K), and albumin (L) was conducted in the cells overlaid with TGP. (I) Enlargement of the portion shown in H indicated by the dotted rectangle. Inset shows a high magnification of the positive nuclei. A phase-contrast photograph of the colony shows that relatively large cells have translucent belts (arrows) between the cells (J). Scale bar, 100 μm. (J and K-M) Phase-contrast micrograph and double immunostaining for MRP2 and albumin of the same cells, respectively. The cells with large cytoplasm are positive for albumin and form translucent belts between the cells. MRP2 is expressed along the belt-like structures. TGF, thermoreversible gelation polymer.

As shown in Table 2, reverse transcription polymerase chain reaction indicated that the isolated cells expressed albumin, transferrin, HNF3α, HNF4, CYP1A1 (hepatic markers), CX43, CK19, CK18 (cholangiocyte markers), AFP, c-Kit, Thy1, and Musashi-1 (immature cell markers).[11] The cells in NT lost the immature cell markers at day 35, and marker genes of differentiated hepatocytes such as TAT, C/EBPα, and CYP2E1 were not detected.

However, when the cultured cells were overlaid with TGP, TAT, C/EBPα, and CYP2E1 genes were expressed at day 35.

Discussion

In rodents and humans, a relationship exists between liver growth and body mass. In resections involving the removal of 40% to 70% of the rodent liver, a linear relationship is seen between the amount of removed tissue and the extent of hepatocyte proliferation. However, the removal of up to 30% of the liver fails to cause a synchronized wave of hepatocyte proliferation after the operation, although the liver eventually regains its mass.[12] In human liver surgery, enucleation of hepatic tumors is performed, and accidental liver injury sometimes occurs. However, the mechanism of the regeneration of a partial defect in the liver is not well understood. Recently, we realized that, when TGP was used as a filler in the partially penetrated liver, we could not find any trace of the injury within 1 month. In the process of hepatic regeneration with TGP, ductular reactions initially appeared at the margins of the area filled with TGP, and the number of inflammatory cells was not large. In addition, although many cells in the ductules showed positive staining of cell cycle–related proteins, proliferation of intact hepatocytes surrounding the injury lesion was relatively few, and the size of the lobules proximal to the lesion did not change after the treatment. This phenomenon was observed only when TGP was used as the filler in the partial defect. When the focal lesion remained untreated (control), exudates immediately filled the space accompanying many inflammatory cells and were then gradually replaced with granulomatous tissue. Even after 1 month, the lesion showed scar formation, and the scar remained for a long time. When FG was used as the filler, a large area of fibrosis in the lesion remained in all rats. Therefore, we considered that the cells in ductular reactions might play an important role in the regeneration of the TGP-treated liver.

The emergence of atypical ductular cells (so-called "ductular reactions") has been reported in some experimental conditions of rodents[13,14] and human liver diseases. For the cellular origin of the ductular reactions, oval cells,[3-5] ductular metaplasia (transdifferentiation from hepatocytes into ductular cells),[13,15] and ductular hepatocytes[3,6,16] have been suggested; however, this is still controversial. In the current experiment, the cells in ductular structures induced by TGP possessed many hepatic proteins such as albumin, transferrin, CYP1A1, HNF3α, and

Table 2. Characterization of the Cells in Ductular Reactions Induced by TGP and the Cultured Cells

Marker Genes	BECs	Cultured Cells (NT)	Isolated Cells	Cultured Cells (TGP)	MHs
Progenitor cells					
Musashi-1	−	−	+	−	−
Oval-cell related					
c-Kit	−	−	+	−	−
Thyl	−	−	+	−	−
AFP	−	−	+	−	−
Hepatocytes					
Albumin	−	+	+	+	+
Transferrin	−	+	+	+	+
TAT	−	−	−	+	+
CYP2E1	−	−	−	+	+
CYP3A1	−	−	−	−	+
Cholangiocytes					
CX43	+	+	+	+	−
CK19	+	+	+	+	−
CK18	+	+	+	+	+
Transcription factors					
HNF3α	−	+	+	+	+
HNF4	−	+	+	+	+
C/EBP α	−	−	−	+	+
HNF6	+	+	+	+	+

NOTE. Gene expression of cell lineage markers was analyzed by semi-quantitative RT-PCR. Total RNA was isolated from BECs (normal rat), the isolated cells in ductular reactions induced by TGP, the cultured cells without overlay (NT) and with TGP (TGP), and MHs (normal rat). Three separate experiments were performed, and the results were reproducible.

−, not detectable; +, detectable.

Abbreviations: BEC, bile epithelial cell; TGP, thermoreversible geiation polymer; NT, no treatment; MH, mature hepatocyte.

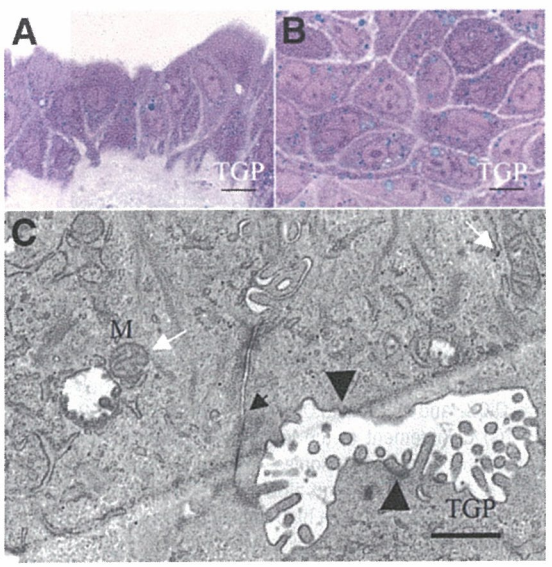

Fig. 5. Perpendicular (A) and horizontal sections (B) of the cultured cells covered with TGP at day 35 (toluidine-blue staining). Hepatocyte-like cells are seen. The size of the cells is between BEC and MH. Scale bars, 10 μm. Ultrastructure of the hepatocyte-like cells at day 35 (C). BC with many microvilli (arrowhead) is shown, and the cytoplasm is rich in organelles such as mitochondria (white arrows) and rough endoplasmic reticulum. A tight junction (an arrow) is observed. Scale bar, 1 μm. TGF, thermoreversible gelation polymer; BEC, bile epithelial cell; MH, mature hepatocyte.

HNF4, which were expressed from the initial day of their appearance, although proteins expressed in cholangiocytes and immature hepatocytes were also co-expressed. The features of the cells were initially very similar to terminal BECs. However, the cells gradually became larger after the injury, and the morphological appearance became similar to that of hepatocytes. The morphological alteration of typical cells was observed in the tips of tubular structures at approximately POD 9. The cellular size was intermediate between typical BECs and MHs. In addition, the hepatocyte-like cells increased in the area where the morphological changes of the cells were observed, such as the area surrounding the ductules. The hepatocyte-like cells could produce glycogen in their cytoplasm, and PAS-positive basement membrane around the cells also disappeared. Conversely, they lost the expression of the marker proteins of BECs and immature cells such as CK19, c-Kit, Thy1, and AFP. The cells with hepatobiliary characteristics seemed to differentiate into MHs. With the reduction of the injured area, hepatocyte-like cells rapidly increased, and most of the injured area was occupied by those cells. These results suggest that the cells induced are quite similar to the ductular hepatocytes that were previously reported. The cells have sometimes been observed after massive (or submassive) hepatic necrosis in rats [3,6,16] and in humans.[17-19] Ductular hepatocytes are considered to be an intermediate form between BECs and MHs, resembling ductal plate cells in the developing human liver. They are located at the periphery of the portal tract, proliferate, and express cholangiocyte and hepatocyte markers. However, it has never clearly been shown that ductular hepatocytes can differentiate into and replace ductules with hepatocytes. Fujita et al.[19] demonstrated by sequential liver biopsies over a period of 14 months that a patient who received an auxiliary partial orthotopic liver transplant after suffering massive necrosis had complete regeneration of natural liver.[19] Therefore, we tried to isolate and culture the intermediate cells from ductular reactions induced by TGP. In addition, we examined whether the cells could differentiate into MHs. In this study, isolated cells co-expressing hepatobiliary cell markers could be purified and cultured for a prolonged period. Although many cell aggregates detached from the dish, some survived and expanded after TGP treatment. The overlay of TGP may prevent detachment and stimulate the expansion of the cultured cells. Histological examinations of the TGP-treated rat livers showed that only the BECs close to TGP could extend processes and differentiate into hepatocytes. The ductules far from TGP never showed ductular reactions. In the current experiment, we isolated the cells in ductules from enucleated liver specimens, which included a large area of the margin (10 mm diameter). The margin may have included non-activated BECs, which TGP might not strongly influence. Such non-activated BECs seemed to decrease. The overlay of TGP may stimulate the selective expansion of the cells influenced by TGP.

Oval cells, which are hepatic progenitor cells, are related to terminal biliary ductules and the so-called canals of Hering.[5,20] They are small cells that have an oval-shaped nucleus and scant cytoplasm containing few organelles.[20,21] The oval cells forming ductular structures are usually surrounded by a continuous basement membrane like BECs. Furthermore, they express phenotypic markers of both immature hepatocytes (AFP) and cholangiocytes (CK7, 8, 18, 19, OV6, GGT).[3-5,20,21] In addition, oval cells are known to express hematopoietic stem cell markers such as c-Kit, Thy-1, and CD34.[4,5] In the current experiment, cells in ductular reactions induced by TGP had a round nucleus and relatively large cytoplasm compared with that of oval cells. Although the cells in the ductules immunohistochemically showed expression patterns of AFP, c-Kit, Thy1, and CK19 similar to those of oval cells, they also expressed hepatic markers such as albumin, transferrin, CYP1A1, and HNF4. These genes were not expressed in the oval cells. In addition, oval cells usually appear when hepatic regeneration is impeded by hepatic toxins or the liver is severely damaged. In this study, only a small part of the liver was injured in normal adult rats, and most hepatocytes were intact, as no toxin was systemically administered. These results clearly suggest that the cells induced by TGP are different from oval cells.

Metaplasia of neighboring hepatocytes (ductular metaplasia) into BECs may occur as a result of TGP treatment. In the current experiment, the existence of ductular reactions in the lesion might have been coincident with the suggestive locations of the portal area, which may have existed before the injury. In addition, before the appearance of the ductular reactions at POD 3, although many dead and injured hepatocytes were observed in the area adjacent to TGP, neither a single nor clustered $CK19^+$-cells were randomly detected in those areas. Conversely, at the time of the initial appearance of the cells in ductular reactions, the size and the features of the nuclei were similar to those of BECs.

Thus, TGP itself may have an effect on certain cells to induce differentiation. Recently, it was reported that TGP might have an effect on the renal differentiation of human bone marrow mesenchymal stem cells.[22] Although there is no direct evidence that TGP can play a key role in stem cell differentiation, TGP treatment may directly or indirectly switch on the signal for hepatic differentiation of stem cells in terminal bile ducts or the canal of

Hering. Thus, further investigation is necessary to clarify the molecular mechanism of hepatic differentiation by TGP.

Acknowledgment: We are grateful to Dr. Atsushi Miyajima (Tokyo University, Tokyo, Japan) and Drs. Yuichi Mori, Hiroshi Yoshioka, and Hideo Sakamaki (Waseda University, Tokyo, Japan) for the generous gifts of the rabbit anti-CK19 antibody and TGP, respectively. We also thank Dr. Yoichi Mochizuki for assistance with TEM and Minako Kuwano, Shigeko Ohnuma, Akiko Hosoyama, Erika Takada, Hiroshi Kohara, Izuru Yokomi, and Tsuneo Igarashi for their technical assistance. We also thank Kim Barrymore for help with the manuscript.

References

1. Nagaya M, Kubota S, Suzuki N, Tadokoro M, Akashi K. Evaluation of thermoreversible gelation polymer for regeneration of focal liver injury. Eur Surg Res 2004;36:95-103.
2. Yoshioka H, Mikami M, Mori Y, Tsuchida E: A synthetic hydrogel with thermoreversible gelation: preparation and rheological properties. J Macromol Sci 1994;A31:113-120
3. Sell S. The role of progenitor cells in repair of liver injury and in liver transplantation. Wound Repair Regen 2001;9:467-482.
4. Fausto N. Liver regeneration and repair: hepatocytes, progenitor cells, and stem cells. HEPATOLOGY 2004;39:1477-1487.
5. Alison MR, Vig P, Russo F, Bigger BW, Amofah E, Themis M, et al. Hepatic stem cells: from inside and outside the liver? Cell Prolif 2004;37:1-21.
6. Sirica AE, Williams TW. Appearance of ductular hepatocytes in rat liver after bile duct ligation and subsequent zone 3 necrosis by carbon tetrachloride. Am J Pathol 1992;140:129-136.
7. Wagers AJ, Sherwood RI, Christensen JL, Weissman IL. Little evidence for developmental plasticity of adult hematopoietic stem cells. Science 2002; 297:2256-2259.
8. Tsanadis G, Kotoulas O, Lollis D. Hepatocyte-like cells in the pancreatic islets: study of the human foetal pancreas and experimental models. Histol Histopathol 1995;10:1-10.
9. Mitaka T, Sato F, Mizuguchi T, Yokono T, Mochizuki Y. Reconstruction of hepatic organoid by rat small hepatocytes and hepatic nonparenchymal cells. HEPATOLOGY 1999;29:111-125.
10. Yang L, Li S, Hatch H, Ahrens K, Cornelius JG, Petersen BE, et al. In vitro trans-differentiation of adult hepatic stem cells into pancreatic endocrine hormone-producing cells. Proc Natl Acad Sci U S A 2002; 99:8078-8083.
11. Miura K, Nagai H, Ueno Y, Goto T, Mikami K, Nakane K, et al. Epimorphin is involved in differentiation of rat hepatic stem-like cells through cell-cell contact. Biochem Biophys Res Commun 2003;311:415-423.
12. Bucher NL. Regeneration of mammalian liver. Int Rev Cytol 1963;15: 245-300.
13. Desmet V, Roskams T, Van Eyken P: Ductular reaction in the liver. Pathol Res Pract 1995;191:513-524.
14. Popper H. The relation of mesenchymal cell products to hepatic epithelial system. In: Popper H, Schaffner F, eds. Progress in Liver Diseases. Philadelphia: W.B. Saunders, 1990:27-38.
15. Michalopoulos GK, Barua L, Bowen WC. Transdifferentiation of rat hepatocytes into biliary cells after bile duct ligation and toxic biliary injury. HEPATOLOGY 2005;41:535-544.
16. Sirica AE. Ductular hepatocytes. Histol Histopathol 1995;10:433-456.
17. Roskams T, De Vos R, Van Eyken P, Myazaki H, Van Damme B, Desmet V. Hepatic OV-6 expression in human liver disease and rat experiments: evidence for hepatic progenitor cells in man. J Hepatol 1998;29:455-463.
18. Haque S, Haruna Y, Saito K, Nalesnik MA, Atillasoy E, Thung SN, et al. Identification of bipotential progenitor cells in human liver regeneration. Lab Invest 1996;75:699-705.
19. Fujita M, Furukawa H, Hattori M, Todo S, Ishida Y, Nagashima K. Sequential observation of liver cell regeneration after massive hepatic necrosis in auxiliary partial orthotopic liver transplantation. Mod Pathol 2000;13:152-157.
20. Paku S, Nagy P, Kopper L, Thorgeirsson SS. 2-Acetylaminofluorene dose-dependent differentiation of rat oval cells into hepatocytes: confocal and electron microscopic studies. HEPATOLOGY 2004;39:1353-1361.
21. Hixson DC, Faris RA, Thompson NL. An antigenic portrait of the liver during carcinogenesis. Pathobiology 1990;58:65-77.
22. Hishikawa K, Miura S, Marumo T, Yoshioka H, Mori Y, Takato T, et al. Gene expression profile of human mesenchymal stem cells during osteogenesis in three-dimensional thermoreversible gelation polymer. Biochem Biophys Res Commun 2004;317:1103-1107.

ELSEVIER

Journal of Hepatology 45 (2006) 90–98

Journal of Hepatology

www.elsevier.com/locate/jhep

Expression of CD44 in rat hepatic progenitor cells

Junko Kon, Hidekazu Ooe, Hideki Oshima, Yamato Kikkawa, Toshihiro Mitaka*

Department of Pathophysiology, Cancer Research Institute, Sapporo Medical University School of Medicine, South-1, West-17, Chuo-Ku, Sapporo 060-8556, Japan

See Editorial, pages 1–4

***Background/Aims*: Small hepatocytes (SHs) are hepatic progenitor cells, but the phenotypical difference between SHs and mature hepatocytes (MHs) has never been demonstrated.**

***Methods*: The profile of gene expression was examined to clarify the difference between SHs and MHs by using a DNA microarray. Genes that were specifically expressed in SHs were identified and RT-PCR analysis of them was performed. Immunocytochemistry for CD44 standard form (CD44s) and variant form 6 (CD44v6) was performed using cultured SHs and the D-galactosamine (GalN)-injured rat liver. From the GalN-treated liver, CD44s $^+$ cells were obtained by sorting and RT-PCR analysis was performed.**

***Results*: Analysis using the DNA microarray and RT-PCR of them revealed restricted expression of CD44s and CD44v6 in SHs. In culture, CD44s appeared at day 3 and increased with the proliferation of SHs. CD44v6 expression was delayed compared to that of CD44s. With GalN-administration, CD44 $^+$ hepatocytes appeared around periportal areas at days 3 and 4 and then decreased. Sorted CD44s $^+$ cells could form colonies and possessed hepatic markers.**

***Conclusions*: CD44 is a specific marker of SHs. The expression of CD44 mRNA and protein is restricted to SHs, and is up-regulated at the time when SHs start to proliferate both in vitro and in vivo.**

***Keywords*: CD44s; CD44v6; Small hepatocytes; Proliferation; Maturation**

1. Introduction

Small hepatocytes (SHs) are a subpopulation of hepatocytes that have high growth potential in culture [1–4]. The cells are less than half the size of mature hepatocytes (MHs), but they possess hepatic characteristics [5,6]. SHs can clonally proliferate to form colonies that survive for more than 5 months in defined medium [5,6] and can differentiate into MHs by interacting with hepatic nonparenchymal cells (NPCs) [7] or as a result of treatment with Engelbreth–Holm–Swarm gel [8]. Thus, we consider that SHs may be 'committed progenitor cells' that can further differentiate into MHs. Although SHs are primary cells that are freshly prepared from rat liver, they can also proliferate after cryopreservation [9].

The molecular mechanisms regulating the characteristics of SHs remain to be elucidated. In addition, their precise origin and location within the liver are not clear because the preparation of purified SHs is difficult and specific markers for SHs have never been identified. Therefore, it is important to identify specific genes and proteins expressed in SHs, especially cell membrane-integrated proteins, because it will be possible to clarify the characteristics of the cells by the methods of cell sorting.

Received 18 May 2005; received in revised form 10 January 2006; accepted 17 January 2006; available online 28 February 2006

* Corresponding author. Tel.: +81 11 611 2111x2390; fax: +81 11 615 3099.

E-mail address: tmitaka@sapmed.ac.jp (T. Mitaka).

Abbreviations:: BECs, biliary epithelial cells; CD44s, CD44 standard form; CD44v, CD44 variant form; C/EBPα, CCAAT/enhancer binding protein α; CYP, cytochrome P450; GalN, D-galactosamine; HA, hyaluronic acid; LECs, liver epithelial cells; MH, mature hepatocyte; NPC, hepatic nonparenchymal cell; SH, small hepatocyte.

0168-8278/$32.00
doi:10.1016/j.jhep.2006.01.029

The CD44 gene encodes for a family of alternatively spliced, multifunctional adhesion molecules that participate in lymphocyte–endothelial cell interactions as lymphocyte homing receptors [10–12], and in adhesion of cells to extracellular matrix [13], T cell activation and adherence [14], and metastasis formation [15]. CD44 standard form (CD44s) is composed of a short cytoplasmic tail, a transmembrane region and two extracellular domains. There are 10 additional exons (v1–v10). Although the expression of CD44 variant forms (CD44v) was initially considered to occur as a result of aberrant splicing in tumor cells, variant expression was subsequently detected in normal cells [16]. The expression of variant forms in hematopoietic cells has been reported [17–19].

In the present study, we found that both CD44s and CD44v6 were expressed in cultured SHs and their expression decreased with the maturation of the cells. Although biliary epithelial cells (BECs) also expressed CD44s, no other epithelial cells within the normal rat liver did. However, when the rat liver was severely injured by D-galactosamine (GalN) treatment, CD44s $^{+}$ epithelial cells appeared near Glisson's capsule in the liver lobules and, by using a specific antibody, the cells could sorted and thereafter cultured. These CD44s $^{+}$ cells expressed hepatic marker genes and could proliferate to form colonies consisting of SHs.

2. Materials and methods

2.1. Isolation and culture of SHs

Male F344 rats (Sankyo Lab Service Corporation, Inc., Tokyo, Japan) weighing 150–200 g were used to isolate hepatic cells by the two-step liver perfusion method of Seglen [20] with some modifications [2]. Briefly, suspensions of liver cells were centrifuged at 50×*g* for 1 min. The supernatant was used to prepare SHs and the precipitate was used to prepare MHs. The details of the isolation and culture procedure were previously reported [7]. After the number of viable cells was counted, cells were plated on dishes (7.5×10^4 cells/35-mm, 10×10^5 cells/100-mm dish; Corning Glass Works, Corning, NY). SH colonies cultured in a 100-mm dish were collected at day 14 and cryopreserved at −80 °C. The details of the method were previously reported [9]. After cryopreservation, SHs were thawed and suspended in the culture medium. To induce the maturation of SHs, they were overlaid with growth factor-reduced Matrigel® (BD Biosciences, Bedford, MA) at day 14 after thawing and the cells were then cultured. The details of the method were previously reported [8].

2.2. DNA microarray

Differences of the expression profiles of SHs and MHs were analyzed using a microarray approach. A DNA microarray spotted with 14,815 cDNAs (Agilent rat cDNA microarray kit) was purchased from Agilent Technologies, Inc. (Palo Alto, CA). Poly(A) $^{+}$ RNAs were prepared using ISOGEN (Nippon Gene, Tokyo, Japan) and mRNAs were prepared using a GenElute™-mRNA miniprep kit (Sigma Chem Co, St Louis, MO). Prepared mRNAs were labeled with Cy5- and Cy3-dUTP by reverse transcription. Analysis of the microarray was performed by Hokkaido System Science (Sapporo, Japan).

2.3. RT-PCR

Total RNA was isolated using ISOGEN. Reverse transcription and PCR amplification (RT-PCR) were performed in a one-step reaction according to the manufacturer's instructions (Invitrogen, San Diego, CA). Sequences of forward and reverse primers used are listed in Table 1. The constitutively expressed gene glycerol 3-phosphate dehydrogenase (GPDH) was also reverse-transcribed in a separate reaction as a qualitative and quantitative control.

2.4. Northern blot analysis

Northern blot analysis was performed as previously reported [21]. Probe labeling and RNA detection were performed according to the manufacturer's instructions for the AlkPhos Direct Labelling and Detection System with CDP-Star (Amersham Biosciences, Piscataway, NJ). For probes, the full-length CD44s and partial 450 bp GPDH fragment were used.

2.5. Western blot analysis

After washing with PBS twice, the cells were dissolved in lysis solution (20 mM Tris–HCl [pH 7.4], 150 mM NaCl, 2.5 mM EDTA, 1% Triton-X100, 1% aprotinin, and 20 mg/ml leupeptin). The cells were kept on ice for 30 min and sonicated. After the sonication, the solution was centrifuged at 22,000×*g* for 20 min. The supernatant was kept at −80 °C until use and the protein content was measured using a BCA assay kit (Pierce, Rockford, IL). Western blot analysis was carried out as previously described [7].

2.6. Immunostaining

Antibodies used for immunostaining are listed in Table 2. SHs in a 35-mm dish were used for immunocytochemistry. After washing with PBS, the cells were fixed in 70% cold ethanol. After blocking with BlockAce (Dainippon Pharmaceuticals Co., Osaka, Japan) for 30 min at RT, cells were incubated with the primary antibody for 60 min at RT. Dishes were rinsed with PBS and subsequently incubated with an Alexa^{488}-conjugated antibody (Molecular Probe, Eugene, OR) for 30 min at RT. In case of double staining, the secondary antibody was applied for 60 min. After washing with PBS, the Alexa^{594}-conjugated antibody (Molecular Probe) was applied for 30 min. Finally, cells were embedded with 90% glycerol including 0.01% *p*-phenylenediamine and 4,6-diamidino-2-phenylindole (DAPI).

For immunohistochemistry, the liver was frozen at −80 °C until use. Then 7-μm-thick sections were prepared and air-dried. The staining procedure used for the sections was the same as for immunocytochemistry. A confocal laser microscope (Zeiss, Jena, Germany) was used for observation.

2.7. D-galactosamine administration

GalN (Sigma; 75 mg/100 g body weight dissolved in PBS) was intraperitoneally given to male F344 rats weighing 150–200 g [22]. The animals were killed 1–5 days after the treatment and their livers were removed. Liver slices were prepared, immediately frozen in liquid nitrogen and kept at −80 °C until use.

2.8. Cell sorting and culture

Four days after GalN treatment, hepatic cells were isolated as described above. The isolated cells were centrifuged at 50×*g* for 1 min. The supernatant was collected and then centrifuged again. After the same procedure was repeated, the supernatant was centrifuged at 150×*g* for 5 min and the pellet was suspended in PBS containing 2 mM EDTA and 0.5% BSA. An anti-CD44 antibody (625 ng/ml) was added and, following incubation for 10 min, cells were washed